ISSN 1330-3651 (Print), ISSN 1848-6339 (Online)
https://doi.org/10.17559/TV-20230105000125
Preliminary communication

Strain Measurement on the Glass-Fiber Reinforced Plastic by Using Optical Measurement System

Ivona KOZAK, Nenad GUBELJAK, Darko DAMJANOVIĆ*, Dražan KOZAK, Mitja KASTREVC

Abstract: This paper deals with experimental determination of the mechanical properties of the fiber glass-reinforced plastic. Nine test samples were made from fiber-glass plastic, where three series with three samples each were with different thickness. All samples were of nominal length 250 mm with fibers of length 50 mm. The width of the specimens was 25 mm, and the thickness was 0,35 mm; 0,8 mm and 1,16 mm, respectively. The samples were subjected to tensile testing on a tensile machine in order to determine the mechanical properties. The force and longitudinal displacement (actuator displacement) were measured on the tensile testing machine, while with the optical measuring system, strains in the transverse direction (perpendicular to the tensioning direction) were measured. The results of the measurements on the tensile test machine, presented in the form of stress-displacement diagrams, are shown first within the same series (equal thickness of the test sample) and then the results are compared for different thicknesses of the test sample. By tensometric measurements, the change of the principal strains over time was determined. The engineering stress-strain curve for all nine test specimens was obtained using the optical measuring system and given in form of diagrams. It was found that the best tensile properties of all considered specimens have test specimens with the largest thickness, which also had glass fibers of knitted structure.

Keywords: fiberglass plastic; mechanical properties; optical measuring system; strain measurement

1 INTRODUCTION (INTRODUCTORY REMARKS)

Fiber-reinforced polymers (FRP) have an excellent strength-weight ratio, durability and anticorrosion properties and thus have been widely used for strengthening structures and components [1]. It is simply a composite material made of polymer matrix and reinforced with fibers. There are practically no areas where they are not used, from all type of transport vehicles, to civil infrastructure, processing equipment, sport equipment etc. [2]. Very nice example of advantages in using of FRP is presented in [3] where authors analysed two concept hoods of small electric vehicle. Besides benefits of smaller mass of FRP composite hood, authors achieved the improvement in terms of lateral, transversal and torsional stiffness in relation to similar steel hood. Besides transport vehicles, composite materials are very often used in pressure vessel and piping design [4, 5] and there are even researches which are dealing with reinforcements in concrete structures as a substitute for steel bars [6] as well as direct mixing of carbon fibres into a cement [7]. This is still in research phase, but in some cases composites are used for many years instead of for example aluminium or steel. Good example is carbon-fiber composite which has a relative stiffness five times that of steel and is often used in aircrafts, automobiles, boat hulls, rocket industry etc. [8]. The mechanical behaviour of FRP largely depends on the mechanical properties of fiber itself but also on the matrix strength [9], especially on the connection between fibers and matrix in cases of enabling stress transfer between them [10]. Taking care about composition and orientation of fibers can affect greatly the mechanical properties and can be adapted to the specific functional tasks of the product [11]. Within this research, FRP, specifically fiber-glass polymer (FGP) which is used in manufacturing of Elan skis is considered. In that sense, energy dissipation of composite as well as dynamic stability of polymer matrix are very important [12] since skis are to be used in cold environment under dynamic loading. From the early days, skis are made from wood and they were heavy and difficult to handle. Wood is also highly anisotropic and sensitive to humidity absorbing the moisture and becomes even heavier, reducing strength and causing distortion. So even in those early days skis were made from various materials, combining wood and aluminium and were further developed with plastic base material and steel edges. The main design objective is to combine good strength and flexibility along the longitudinal axis with adequate torsion strength. Also, as it is mentioned, it is necessary to suppress vibrations of wide range of frequency since in operation the skis are subjected to variable dynamic loads at multiple impact points [13]. So taking into account all mentioned, FRP is ideal material for this purpose. Of course, skis are not made fully from FRP, in fact, skis are made as sandwich construction where FRP is just one of used materials in conjunction with metal and often carbon as well [14]. Skis can be made from even 15 layers of different materials [15]. In case of getting full field deformation, optical methods can be applied. In that sense, optical measurement system is the most represented [16-19]. Within this research, specimen thickness is varied in order to analyse the dependency to the tensile strength. This kind of influence is analysed also by other authors for example on samples made from FGP by 3D printing technology [20].

2 EXPERIMENTAL ANALYSIS

For experimental determination of the mechanical properties of the fiber glass-reinforced plastic, two methods are selected: standard tensile test on tensile machine and optical measurement system.

2.1 Specimens Preparation and Designation

Composite material selected for the analysis is made from polymer reinforced with fiber-glass SiOx of 50 mm length. Nominal length of each specimen is l = 250 mm. Each specimen has rectangular cross section with nominal width h = 25 mm, and thickness from b = 0,35 mm (specimen with designation U2); b = 0,8 mm (specimen with designation U3) and b = 1,16 mm (specimen with

designation U4). Three specimens are made for each group U2, U3 and U4, so in total, 9 specimens where tested. The test specimens were not cut directly from the skis, but were made specially from the same material from which the skis are made. Designations of each specimen with its real dimensions and cross sectional area A are presented in Tab. 1.

Table 1 Specimens designations and dimensions

Specimen designation		b / mm	h / mm	A / mm^2
U2	U2_1	0,34	25,03	8,51
	U2_2	0,34	24,43	8,31
	U2_3	0,35	25,49	8,92
U3	U3_1	0,83	24,85	20,63
	U3_2	0,83	22,70	18,84
	U3_3	0,80	25,17	20,14
U4	U4_1	1,16	24,64	28,58
	U4_2	1,15	24,89	28,62
	U4_3	1,15	24,90	28,64

2.2 Microscopic Analysis of Fiber-Glass Reinforcement within Each Group of Specimen

After chemical preparation of the surface of the selected specimens, specimens are analyzed with stereo microscope using magnifications 12×, 25× and 45×. Fig. 1 shows surfaces of one specimen from each testing group U2, U3 and U4 using magnification of 12×.

All the specimens are loaded in axial direction which is in the direction of scale presented in Fig. 1 on each microscopic image. It is obvious that specimens from each testing group U2, U3 and U4 have different reinforcement structure within the matrix. In order to precisely determine structure and its dimensions, thickness of fibers, distance from fibers as well as thickness of matrix between them has been measured. Example of this dimensional analysis for specimen from U3 testing group and for magnifications of 12×, 25× and 45× is presented in Fig. 2.

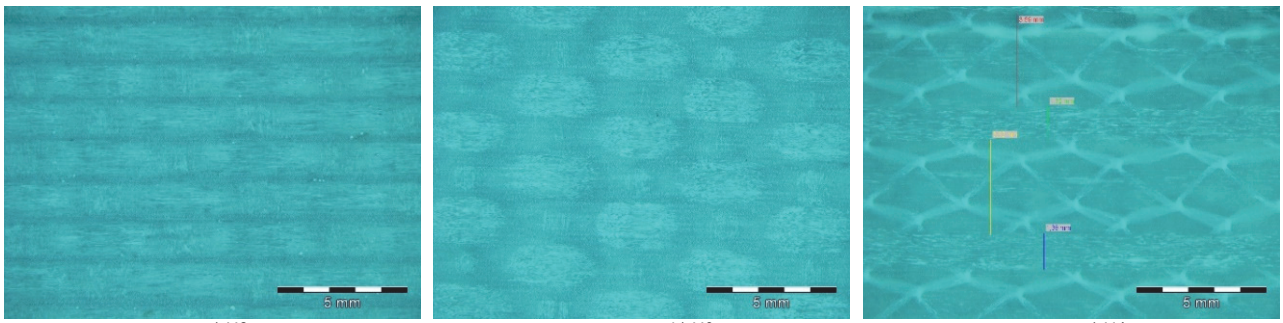

a) U2 b) U3 c) U4

Figure 1 Surfaces of specimens from each testing group (magnification 12×)

Although every testing group has one specific thickness b, not only the influence of thickness on mechanical properties is compared, but also the influence of the structure of individual reinforcement setup. Therefore, optical microscope is used in order to get surface images with magnification of 1000×, Fig. 3. From this analysis it is concluded that some fiber reinforcement has knitted structure (U4), Fig. 3, c).

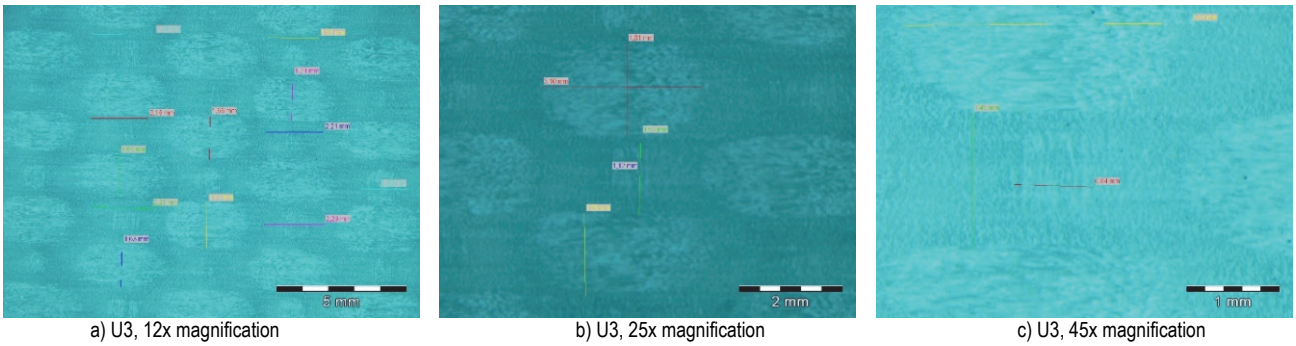

a) U3, 12x magnification b) U3, 25x magnification c) U3, 45x magnification

Figure 2 Fiber thickness and the distance between them for specimen from U3 testing group

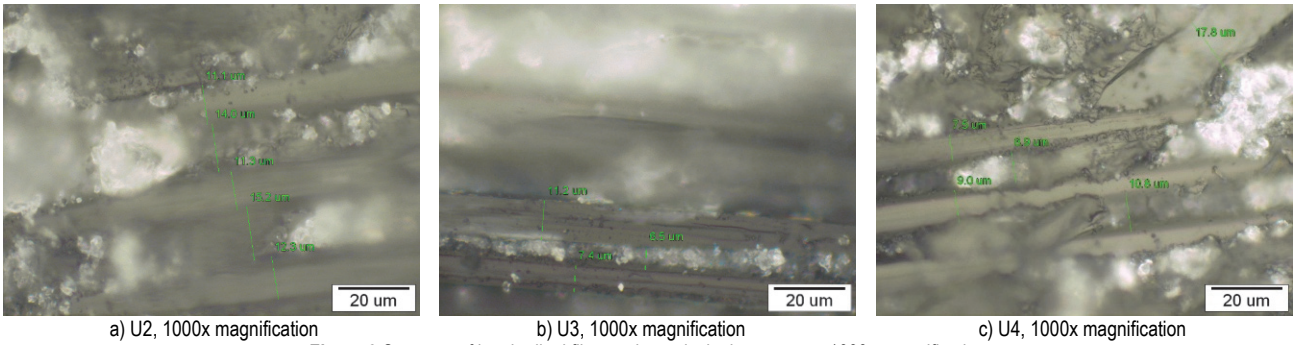

a) U2, 1000x magnification b) U3, 1000x magnification c) U4, 1000x magnification

Figure 3 Structure of longitudinal fiber under optical microscope at 1000× magnification

2.3 Tensile Test

For the purpose of mechanical testing of specimens, tensile test machine is used. The tensile test has been performed according to the ISO 527-1 [21]. Measurement is performed by controlling the displacement with rate 4 mm/min, Fig. 4.

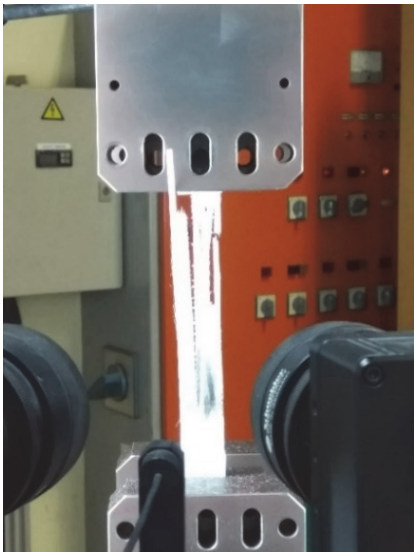

Figure 4 Example of tested specimen within tensile machine clamps

Results of tensile tests for each testing group U2, U3 and U4 are presented, Fig. 5 to Fig. 7.

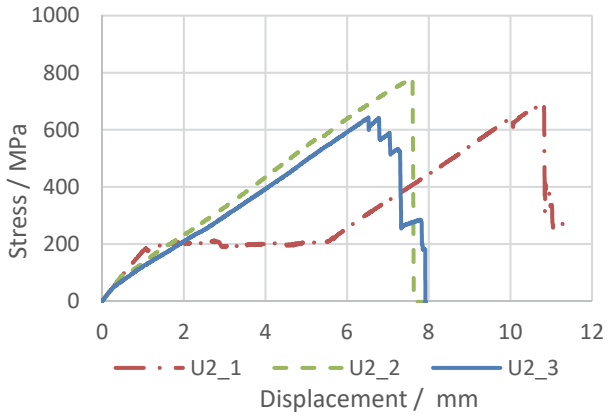

Figure 5 Stress-displacement diagrams within the same testing group U2

There is similar behavior of U2_2 and U2_3 specimens within this testing group, while specimen U2_1 has initially similar slope as well, but after that there is displacement of almost 5 mm without increase of stress at all. So there is significant yielding and after that again increase of stress.

Fig. 6 shows results in means of stress displacement curves within the testing group U3.

Here is practically the same situation as in testing group U2. So one can notice also very similar behavior of U3_2 and U3_3 specimens, while specimen U3_1 has initially similar slope as well, but after that there is displacement of almost 7 mm without increase of stress at all. Here within U3 testing group, maximal reached stresses are significantly lower in relation to the testing group U2.

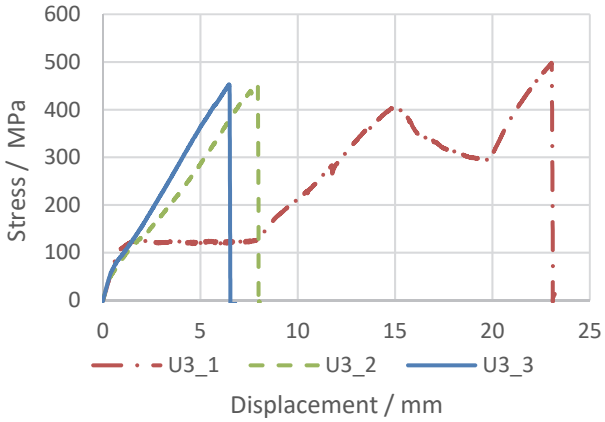

Figure 6 Stress-displacement diagrams within the same testing group U3

Fig. 7 shows stress displacements curves for testing group U4. Here, specimens U4_2 and U4_3 show very similar behavior, while specimen U4_1 has obviously slightly higher stiffness. Maximal reached stresses are expected to be greatest for the specimens with highest thickness considered within this research (1,16 mm), and they are doubled in relation to the specimens with thickness of 0,8 mm.

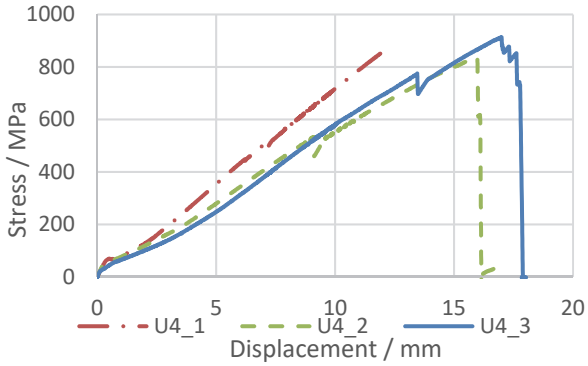

Figure 7 Stress-displacement diagrams within the same testing group U4

2.5 Measurement with Optical Measurement System

On all specimens within this research, optical measurement system is also performed. Example of measurement on specimen U2_1 is presented in Fig. 8 in 130th second from beginning of measurement.

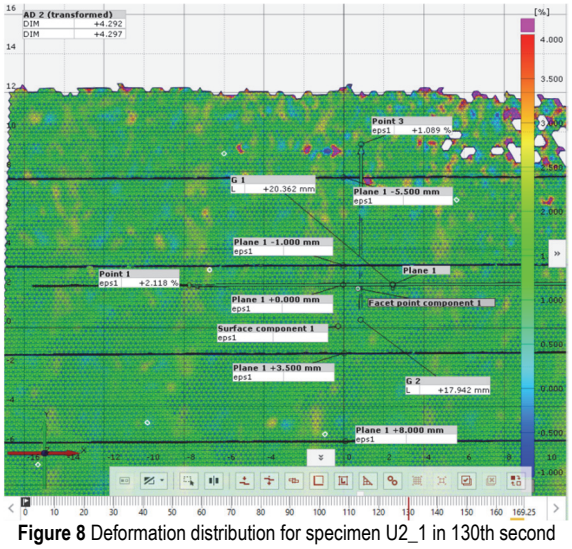

Figure 8 Deformation distribution for specimen U2_1 in 130th second

For specimen U2_1 at the beginning of the measurement, reference points $G_{1,L}$ = 20,035 mm and $G_{2,T}$ = 18,023 mm are taken into account. At the end of the measurement (t = 169,25 s) new coordinates of those reference points are $G_{1,L}$ = 20,514 mm and $G_{2,T}$ =17,898 mm. Considering coordinate changes of reference points, i.e. position changes, it is possible to obtain principal strain in longitudinal direction of specimen (ε_1), and in transversal direction (ε_2). From those data it is possible to calculate the Poisson's ratio.

Fig. 9 shows conventional curves σ-ε obtained with optical measuring system for all nine specimens. From diagram in Fig. 9 it can be noticed that the specimens from U3 testing group have the worst properties, slightly better are specimens from U2 testing group while the best are for specimens from U4 testing group. Specimens from U4 testing group have the greatest thickness but also they have glass fibers of knitted structure.

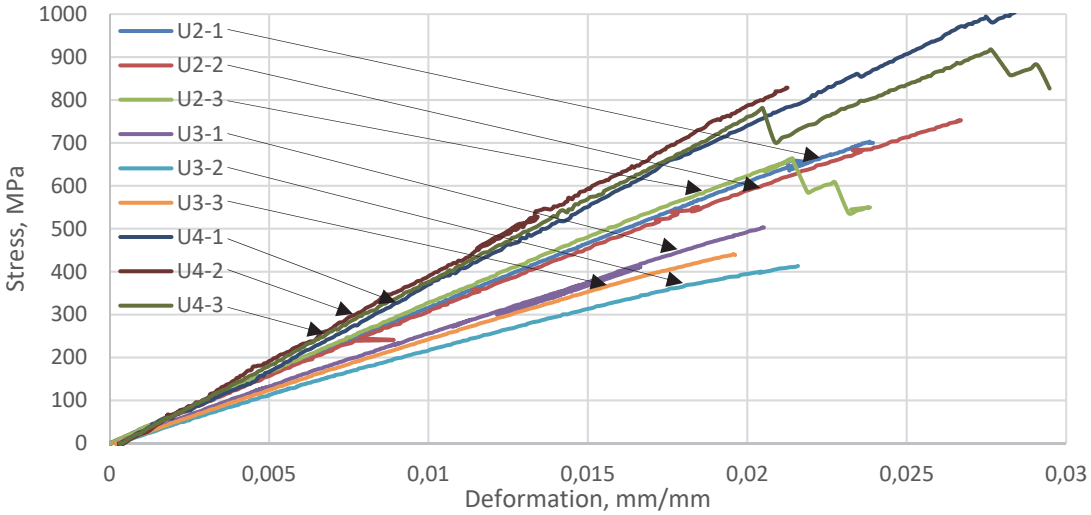

Figure 9 Conventional curves σ-ε obtained with optical measurement system

2.6 Determination of Mechanical Properties

The main aim of this paper is to determine the constant of elasticity of composite material in means of Young's modulus of elasticity E, Poisson's ratio ν and shear modulus G. Of course, it is needed to determine E and ν while G can be calculated from them.

Young's modulus of elasticity for each specimen is determined from conventional σ-ε diagrams obtained by optical measuring system (Fig. 9). Young's modulus is determined from slope of linear-elastic part of each diagram. Fig. 10 shows linear-elastic part of conventional σ-ε diagram for specimen U2_1 where Young's modulus of elasticity can be obtained from relation $E = \tan\alpha$. The points E-Start and E-End are chosen for the most linear part of the curve.

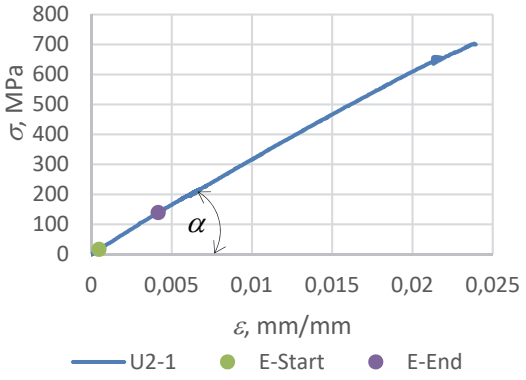

Figure 10 Linear-elastic part of σ-ε diagram for specimen U2_1 obtained by optical measurement system

All the obtained values for Young's modulus of elasticity as well as corresponding values of tensile strength are presented in Tab. 2 for each specimen.

To experimentally determine the Poisson's ration, it is needed to monitor longitudinal and transversal deformation what is done within this research with optical measuring system. Since Poisson's ratio is not constant it is possible to present it as a function of longitudinal displacement. In that sense, Poisson's ratio versus longitudinal displacement for specimen U2_1 is presented in Fig. 11.

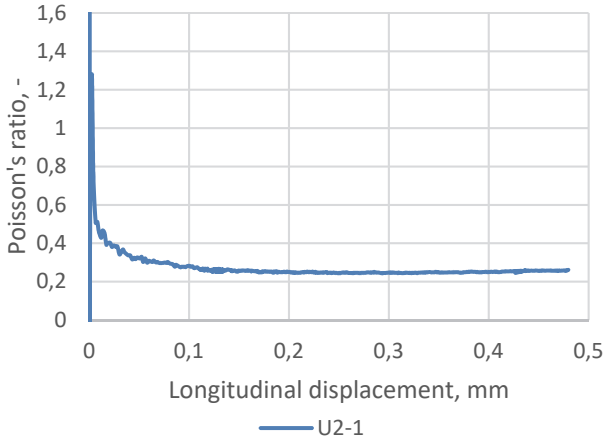

Figure 11 Poisson's ratio in dependence on longitudinal deformation for specimen U2_1

Mean values for Poisson's ratio are calculated for each specimen and presented in Tab. 2. Mean values are calculated from data where the Poisson's ratio value

becomes almost constant, for example on specimen U2_1 in Fig. 11 from 0,1 of longitudinal displacement.

Shear modulus can be calculated from very well-known relation which connects elasticity modulus, shear modulus and Poisson's ratio. All calculated shear modulus values are presented in Tab. 2.

To summarize, all the calculated values for mechanical properties for each specimen are presented in Tab. 2.

Table 2 Mechanical properties of each considered specimen

Specimen designation		E / GPa	G / GPa	ν/	R_m / MPa
U2	U2_1	33,68	13,47	0,25	702,9
	U2_2	31,30	12,93	0,21	752,8
	U2_3	31,97	12,79	0,25	663,3
U3	U3_1	26,59	12,09	0,10	503,3
	U3_2	23,07	10,12	0,14	413,3
	U3_3	24,38	10,60	0,15	440,8
U4	U4_1	31,88	12,65	0,26	1013
	U4_2	39,00	15,60	0,25	828,5
	U4_3	38,61	15,32	0,26	917,4

By analyzing the results, it can be noticed that the largest values of Young's modulus of elasticity E are for specimens from testing group U4 what is expected due to the maximal thickness as well as structure of fibers. Same situation is with Poisson's ratio, so the greatest value is for specimens from testing group U4, what is again expected due to the maximal thickness as well as structure of fibers.

3 CONCLUSIONS

The aim of this study was to determine the mechanical properties of glass fiber reinforced polymer by cutting nine test specimens of different thickness from the ski material. All specimens were subjected to tensile testing on a tensile machine where force and longitudinal displacement (actuator displacement) were measured.

It was found that the worst mechanical properties were shown by the test specimens from the U3 testing group, while the best properties were shown by the test specimens from the U4 testing group which has the largest thickness of the specimens and which also had glass fibers of knitted structure.

Future research on FGP test specimens made from ski material will focus in depth on reinforcement analysis. It should be noted here that even this research shows that thickness clearly has effect on the properties, actually it could happen that the thickness has no effect, except on the different reinforcement along it.

4 REFERENCES

[1] Teng, J. G., Chen, J. F., Smith, S. T., & Lam, L. (2002). *FRP-Strengthened RC Structures.* Oxford, John Wiley and Sons.

[2] Rangappa, M. S., Rajak, K. D., & Siengchin, S. (2022). *Natural and Synthetic Fiber Reinforced Composites: Synthesis, Properties, and Applications, First Edition*. Wiley.

[3] Bere, P., Dudescu, M., Neamtu, C., & Cocian, C. (2021). Design, Manufacturing and Test of CFRP Front Hood Concepts for a Light-Weight Vehicle. *Polymers*, *13*, 1374. https://doi.org/10.3390/polym13091374

[4] Yarrapragada, R., Mohan, K. R., & Kiran,V. B. (2012). Composite pressure vessels. *International journal of Research in Engineering and Technology*, *1*(4).

[5] Bere, P., Nemes, O., Dudescu, C. M., Berce, P., & Sabau, E. (2013). Design and Analysis of Carbon/Epoxy Composite Tubular Parts. *Advanced Engineering Forum*, *8-9*, 207-214. https://doi.org/10.4028/www.scientific.net/AEF.8-9.207

[6] Shamim, A. S. & Kharal, Z. (2018). Replacement of steel with GFRP for sustainable reinforced concrete. *Construction and Building Materials*, *160*, 767-774. https://doi.org/10.1016/j.conbuildmat.2017.12.141

[7] Demir, I., Sevim, O., Ogdu, M. K., Dogan, O., & Demir, S. (2021). Mechanical and Physical Properties of Autoclaved Aerated Concrete Reinforced Using Carbon Fibre of Different Lengths. *Tec*hnical Gazette, *28*(2), 503-508. https://doi.org/10.17559/TV-20200218194755

[8] Masuelli, M. A. (2013). Fiber Reinforced Polymers. *Intech Open*. https://doi.org/10.5772/54629

[9] Štefić, T., Jurić, A., & Marović, P. (2011). Determination of modulus of elasticity for glass fibre reinforced polymers. *Technical Gazette*, *18*(1), 69-72.

[10] Erden, S., Sever, K., Seki, Y., & Sarikanat, M. (2010). Enhancement of the mechanical properties of glass/polyester composites via matrix modification glass/polyester composite siloxane matrix modification. *Fibers and Polymers*, *11*, 732-737. https://doi.org/10.1007/s12221-010-0732-2

[11] Chen, M., Chaoying, W., Yong, Z., & Yinxi, Z. (2004). Fibre Orientation and Mechanical Properties of Short Glass Fibre Reinforced PP Composites. *Polymers and Polymer Composites*, *13*(3), 253-262. https://doi.org/10.1177/096739110501300305

[12] Sathishkumar, T., Satheeshkumar, S., & Naveen, J. (2014). Glass fiber-reinforced polymer composites a review. *Journal of Reinforced Plastics and Composites*, *33*(13), 1258-1275. https://doi.org/10.1177/0731684414530790

[13] Casey, H. (2001). Materals in ski design & development. *Materials and science in sports, TMS*, 11-17.

[14] Poodts, E., Panciroli, R., & Minak, G. (2013). Design rules for composite sandwich wakeboards. *Composites*, *44*(1), 628-638. https://doi.org/10.1016/j.compositesb.2012.02.014

[15] Bozak, T., Muller, M., Kolar, V.,Tichy, M., Svobodova, J., & Michna, S. (2022). Research on Low-Cycle Fatigue Engineered Hybrid Sandwich Ski Construction. *Polymers*, *14*, 2278. https://doi.org/10.3390/polym14112278

[16] Koke, I., Muller, W. H., Ferber, F., Mahnken, R., & Funke, H. (2008). Measuring mechanical parameters in glass fiber-reinforced composites: Standard evaluation techniques enhanced by photogrammetry. *Composites Science and Technology*, *68*(5), 1156-1164. https://doi.org/10.1016/j.compscitech.2007.08.026

[17] Barnefske, E., Keller, F., Gehmert, C., & Sternberg, H. (2016). A Comparison of Strain Measurement Systems in a Tensile Experiment. *Conference: FIG Working Week*, 2016, New Zeland.

[18] Milosevic, N., Younise, B., Sedmak, A., Travica, M., & Mitrovic, A. (2021). Evaluation of true stress-strain diagrams for welded joints by application of Digital Image Correlation. *Engineering Failure Analysis*, *128*, 105609. https://doi.org/10.1016/j.engfailanal.2021.105609

[19] Sedmak, A., Milosevic, M., Mitrovic, N., Petrovic, A., & Maneski, T. (2012). Digital Image Correlation in experimental mechanical analysis. *Structural Integrity and Life*, *12*, 39-42.

[20] Bochina, J., Blasiak, M., & Kozior, T. (2020). Tensile Strength Analysis of Thin-Walled Polymer Glass Fiber Reinforced Samples Manufactured by 3D Printing Technology. *Polymers*, *12*. https://doi.org/10.3390/polym12122783

[21] Plastics-Determination of tensile properties (2012). ISO copyright office, Switzerland.

Contact information:

Ivona KOZAK, univ. bacc. ing. mech.
Faculty of Engineering, University of Rijeka
Vukovarska 58, 51000 Rijeka, Croatia
E-mail: ikozak@riteh.hr

Nenad GUBELJAK, Full. Prof.
Faculty of Mechanical Engineering, University of Maribor
Smetanova 17, 2000 Maribor, Slovenia
E-mail: nenad.gubeljak@um.si

Darko DAMJANOVIĆ, Assist. Prof.
(Corresponding author)
Mechanical Engineering Faculty in Slavonski Brod, University of Slavonski Brod
Trg Ivane Brlic-Mazuranic 2, 35000 Slavonski Brod, Croatia
E-mail: ddamjanovic@unisb.hr

Dražan KOZAK, Full. Prof.
Mechanical Engineering Faculty in Slavonski Brod, University of Slavonski Brod
Trg Ivane Brlic-Mazuranic 2, 35000 Slavonski Brod, Croatia
E-mail: dkozak@unisb.hr

Mitja KASTREVC, Assist. Prof.
Faculty of Mechanical Engineering, University of Maribor
Smetanova 17, 2000 Maribor, Slovenia
E-mail: mitja.kastrevc@um.si